Mechanistic Insights into Methanol-to-Olefin Reaction on an α-Mn_2O_3 Nanocrystal Catalyst

Jing Xu, Like Ouyang, Yan Luo, Xi-Meng Xu, and Zhen Yang
State Key Laboratory of Chemical Engineering, East China University of Science and Technology, Shanghai 200237, China

Chengxi Zhang and Jinlong Gong
Key Laboratory for Green Chemical Technology of Ministry of Education, School of Chemical Engineering and Technology, Tianjin University, Tianjin 300072, China

Yi-Fan Han
State Key Laboratory of Chemical Engineering, East China University of Science and Technology, Shanghai 200237, China

DOI 10.1002/aic.13725
Published online January 17, 2012 in Wiley Online Library (wileyonlinelibrary.com).

The synthesis and utilization of an α-Mn_2O_3 nanocrystal catalyst for methanol-to-olefin reaction is described. A methanol conversion of 35% and a maximum selectivity of 80% toward ethylene were obtained at 250°C. In particular, formaldehyde, a primary intermediate for the reaction, was used to produce ethylene via a coupling reaction. A conversion of 45% and a selectivity of 66% to ethylene were achieved at 150°C in a formaldehyde stream. In situ *diffuse reflectance infrared Fourier transform spectra reveal the formation of the surface CH_2-containing species during reaction, which implies that the main pathway for formaldehyde coupling is probably through interactions of those intermediates. In addition, the weakly adsorbed oxygen on the α-Mn_2O_3 nanocrystal surface was found to play an important role in this reaction.* *AIChE J,* 58: 3474–3481, 2012
Keywords: methanol-to-olefin, ethylene production, formaldehyde coupling, α-Mn_2O_3 nanocrystals, in situ *diffuse reflectance infrared Fourier transform spectroscopy*

Introduction

Ethylene, as a key building block widely used for making polymers, is currently produced via steam cracking of alkanes,[1] which is an energy-intensive process accounting for approximately 70% of the U.S. olefins output. About 3.0% of the total U.S. energy is consumed for the production of chemicals. Recently, the growing demands for crude oil and general energy in industry cause the uprising of traditional feedstock prices for light olefin. Therefore, great efforts have been contributed to develop new processes by using cheap, abundantly available, and renewable raw materials such as coal and biomass to substitute for crude oil.

Several alternative processes[2–5] as illustrated in Scheme 1 have been developed for ethylene production. Among them, olefin production from methanol [methanol-to-olefin (MTO)] is the most promising replacement as well as being ready for commercial use. The advantages of this process include that: (1) methanol can be produced massively from syngas (CO and H_2), which can be derived directly from coal, natural gas, and biomass, (2) methanol has also proved to be synthesized directly from catalytic oxidation of methane, and (3) a high selectivity toward olefin in converting methanol (about 49% ethylene, 30% propylene, and 10% butylenes) makes the methanol-based route, noncrude oil materials (coal, natural gas, and biomass) → syngas → methanol → ethylene, to be economically attractive.[6,7] A further simple way to produce ethylene is through the dehydrogenation of ethane, which can be created by the coupling of methane.

In addition, the consumption of ethylene is expected to increase significantly because of the growing demand for ethanol, which may be produced potentially from ethylene hydration.[8] Ethanol is now accepted well as an eco-friendly biofuel compared with methanol.

Currently, the MTO reaction is mainly carried out by using acidic zeolite catalysts such as modified Hydrogen-Zeolite Socony Mobile-5(H-ZSM-5) and silicoaluminophosphate (SAPO). The mechanism studies about this reaction system have been recently reviewed in detail,[9] whereas dimethyl ether, methane/formaldehyde, and other C_1 species were proposed as intermediates.[10,11] Unfortunately, there is no clear-cut reaction route of ethylene formation unanimously accepted because the theoretical calculations are generally inconsistent with the experimental observations.

On the other hand, highly selective catalyst for this reaction is demanded for industry, which will further improve the utilities of raw materials and lower the cost of olefins.

Additional Supporting Information may be found in the online version of this article.

Correspondence concerning this article should be addressed to Y.-F. Han at yifanhan@ecust.edu.cn and J. Gong at jlgong@tju.edu.cn.

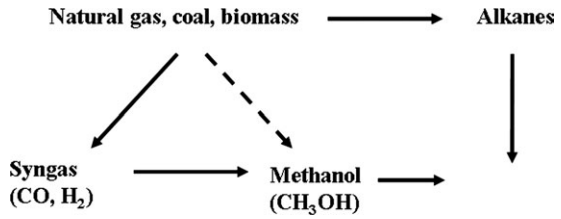

Scheme 1. Practical (solid line) and potential processes (dash line) for ethylene production

Up to now, the MTO reaction on oxide catalysts has received less attention except for limited information driven from model catalysts such as TiO_2 powder[12] and $UO_2(111)$ single crystals.[13] In this study, for the first time we report that α-Mn_2O_3 nanocrystals can be a potential selective catalyst for this reaction. We attempt to provide mechanistic insights into the relatively high selectivity toward ethylene.

Experimental

Catalyst preparation

α-Mn_2O_3 nanocrystals were prepared by direct oxidative decomposition of $MnCO_3$ powder (99.9%, Aldrich) in static air. $MnCO_3$ powder was calcined at 500°C for 5 h with a ramping rate of 1°C min^{-1}. The as-prepared nanocrystals show a mean particle size of 30.0 nm in diameter (d_p) [measured by both scanning electronic microscopy (SEM) and X-ray diffraction (XRD)] and a surface area of 40 m^2 g^{-1} (S_{BET}). A reference bulk α-Mn_2O_3 (Aldrich, 99.999%, ~0.5 μm, 4.8 m^2 g^{-1}) is commercially available. The preparation method has been introduced in detail in our previous studies.[14–17]

Characterization

Scanning Electronic Microscopy. The measurements were performed on a JEOL JSM-6700F Field Emission SEM. About 200 particles were selected to estimate particle-size distribution.

X-ray Diffraction. XRD patterns were recorded with a Bruker D8 diffractometer using CuK_α radiation (λ = 1.540589 Å). The crystal size of MnO_x was calculated with the width of diffraction profiles, referring to the full width of half maximum (FWHM) of crystalline phase at ⟨222⟩, ⟨440⟩, and ⟨622⟩ using Debye–Scherrer formula:

$$D = 0.9 \times \lambda/\Delta \times \cos(\theta) \quad (1)$$

where D is the crystal size, λ is the wavelength of X-ray, Δ is the FWHM of diffraction peak, and θ is the angle corresponding to the peak.

HCHO-Temperature-Programmed Desorption. Temperature-Programmed Desorption (TPD) experiment was performed using a micro-fixed-bed reactor (quartz reactor with 20-cm long and 0.4-cm diameter) connected to a Gas Chromatograph-Quadrupole Mass Spectrometer (GC-QMS) (HPR-20, Hiden Analytical), where masses (*m/e*: 2(H_2), 15(CH_4), 18(H_2O), 25(C_2H_2), 27(C_2H_4), 28(CO, N_2), 29(HCHO), 30(C_2H_6), 31(CH_3OH), 32(O_2), 44(CO_2), 45(HCOOH)) were monitored. HCHO was introduced into the system by bubbling 37% HCHO aqueous solution [Fisher Scientific (A.P.)] at 2°C for 10 min each time; the partial pressure of HCHO in the gas phase was about 0.14 kPa. The system was then purged with N_2 (50 ml min^{-1}) for 10 min again. The temperature ramped from 25 to 500°C with a rate of 20°C min^{-1} in N_2 (50 ml min^{-1}).

O_2-Temperature-Programmed Desorption. O_2-TPD experiments started with the oxygen-precovered catalysts. Adsorbents of O_2 [O_2 (5%)–He flow of 50 ml min^{-1}] were introduced into the system at 275 K for 30 min. Then, the system was purged with N_2 (50 ml min^{-1}) for 10 min. The temperature ramped from 25 to 500°C with a rate of 20°C min^{-1} in N_2 (50 ml min^{-1}).

Temperature-Programmed Surface Reaction. Temperature-Programmed Surface Reaction (TPSR) spectra were obtained from oxygen-precovered α-Mn_2O_3 in a stream of 0.14 kPa HCHO, 5.0 kPa O_2, 2.6 kPa H_2O, and remaining He with a total flow rate of 50 ml min^{-1} and a ramping rate of 20°C min^{-1}.

N_2 Adsorption. N_2 adsorption and desorption isotherms were collected on an Autosorb-6 at −198°C. Prior to the measurements, all samples were degassed at 300°C until a stable vacuum of about 5 mTorr was reached.

Diffuse Reflectance Infrared Fourier Transform Spectroscopy. In situ diffuse reflectance infrared Fourier transform spectroscopy (DRIFT) of HCHO adsorption on α-Mn_2O_3 nanocrystals was conducted in an reaction cell (modified Harricks model HV-DR2) to allow gas flowing continuously through the catalyst bed (ca. 0.1 g) during spectra acquisition. The spectra were recorded on a PerkinElmer FTIR 100 (resolution: 4 cm^{-1}) spectrometer. Contributions from gas-phase HCHO were eliminated by subtracting the corresponding spectra from the pure KBr powder. Preparing the oxygen-precovered surface and adsorbing HCHO followed the same procedure as described in the TPD experiments.

Activity measurements

Methanol to Ethylene. Methanol dehydration was carried out in a vertical fixed-bed microreactor under atmospheric pressure. In a typical experiment, the catalyst is packed between two layers of quartz wool in the reactor and treated in air flow (50 ml min^{-1}) for 4 h at 500°C. The reaction temperature was monitored by a thermocouple with its tip located in the catalyst bed and connected by a Proportion Integration Differentiation (PID)-type temperature indicator controller. Catalytic tests were performed by injecting methanol and its diluted solutions with a High Performance Liquid Chromatograph (HPLC) infusion pump (Agilent 1100 series). The gaseous products, after the catalyst had attained a steady state, were analyzed using an online gas chromatography (Agilent 6890) equipped with a flame ionization detector using a HP-5 capillary column and a thermal conductivity detector using a Hayesep D column. Liquid products were condensed at 0°C and analyzed with a gas chromatography–mass spectroscopy (Agilent 6890). The reaction was operated in the feed gas of 10.0 kPa CH_3OH, 2.6 kPa H_2O, 0.01 kPa O_2, and remaining He, and a space velocity of 60,000 h^{-1} under atmospheric pressure (the catalyst amount of 50 mg and the flow rate of 50 ml min^{-1}). The conversion of methanol and the selectivity to ethylene calculated by Eqs. 2 and 3 are as follows

$$X_{CH_3OH} = \frac{N_{CH_3OH,i} - N_{CH_3OH,j}}{N_{CH_3OH,i}} \times 100 \quad (2)$$

$$S_E = \frac{2 \times N_{E,j}}{\sum N_{E,i}} \times 100 \quad (3)$$

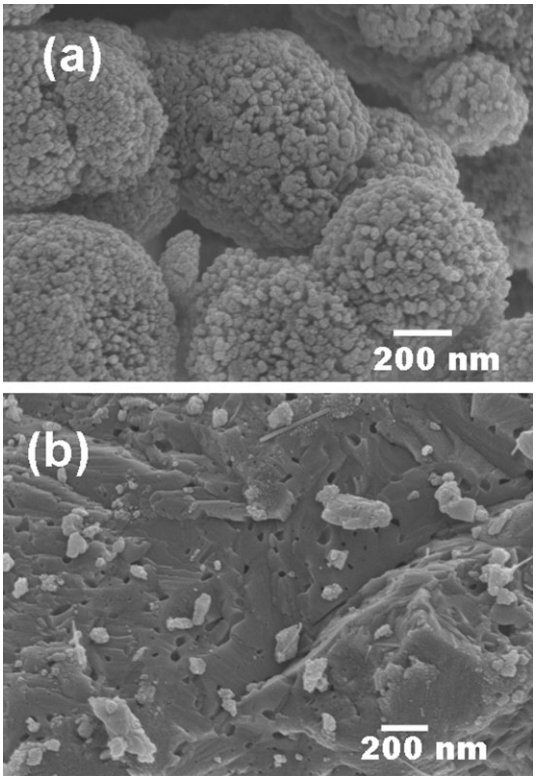

Figure 1. SEM images of α-Mn_2O_3 nanocrystals (a) and bulk α-Mn_2O_3 (b).

X_{CH_3OH} is molar conversion of methanol, $N_{CH_3OH,i}$ is mol of methanol introduced, $N_{CH_3OH,j}$ is mol of methanol in the products, S_E is selectivity toward ethylene in % mol, $N_{E,j}$ is the mol of ethylene in the products, and $\sum N_{E,i}$ is total mol of methanol consumed during reaction.

Absolute mass-specific reaction rates (Eq. 4) were calculated for the average concentration of each component, $\dot{c}_i$, at the inlet and outlet of the reactor. Equation 4 was used for calculating the differential rates for reactions of the MTO and formaldehyde to ethylene, while the initial conversion (at 5 min) was controlled within 10% by diluting with α-Al_2O_3

$$r_{CH_3OH/HCHO} = \frac{\dot{c}_{CH_3OH/HCHO,in} \cdot X_{CH_3OH/HCHO} \cdot \dot{V}_{gas}}{m_{Mn_2O_3} \cdot S_{BET}} \times [\text{mol} \cdot \text{s}^{-1} \cdot m_{Mn_2O_3^{-2}}] \quad (4)$$

Formaldehyde to Ethylene. As the same abovementioned method, the catalyst was pretreated prior to the experiments in O_2 (5%)–He flow. Thus, treated sample, namely, oxygen-precovered surface is ready for the adsorption/reaction experiments.

The temperature-dependent reactivity was obtained in the feed gas of 0.14 kPa HCHO, 2.6 kPa H_2O, and remaining He, with a space velocity of 60,000 h^{-1} under atmospheric pressure. The effluents were analyzed with an online mass spectroscopy. A standard gas (2.5 kPa ethylene in He) was used for ethylene calibration. The concentration of HCHO was calculated according to saturated vapor pressure. The reaction was also carried out in the same system connected to an online rapid-response micro-gas chromatograph (Agilent 3000A micro-GC), whereas ethylene as the only gas-phase product was quantitatively determined.

Selectivity of ethylene (%) = (mol of formaldehyde to ethylene/mol of total conversion of formaldehyde) × 100.

Yield of ethylene (%) = (mol of formaldehyde to ethylene/mol of total input of formaldehyde) × 100.

Results and Discussion

Surface morphology and crystallite phases of the bulk and nanosized Mn_2O_3 were implemented using SEM (Figure 1) and XRD (Figure 2). It is clear that α-Mn_2O_3 crystal phase is dominant in nanoparticles with a coral-like feature. We have first examined the MTO reaction over both bulk ($\bar{d}_{crystal}$: ~500 nm, S_{BET}: 4.8 m^2 g^{-1}) and nanocrystal α-Mn_2O_3 ($\bar{d}_{crystal}$: ~30.0 nm, S_{BET}: 40 m^2 g^{-1}) catalysts. Figure 3a shows that methanol conversion increases with the temperature. The reaction started at 125°C and the conversion reached to 35% at 250°C with a maximum selectivity of 80% toward ethylene. Formaldehyde was identified as the primary byproduct with a maximum selectivity of about 10% at 200°C. Formaldehyde was likely produced through the partial oxidation of methanol. Meanwhile, the corresponding temperature-dependent rates (differential) in a temperature range 100–250°C were illustrated in Figure 3b; the apparent activation energy (E_a) was estimated to be about 25.6 kJ mol^{-1}. The overall carbon balance below 250°C was approached to 98.2% with the evaluation of the concentrations of methanol, formaldehyde, CO_2, and carbon deposit by subsequent Temperature-Programmed Oxidation (TPO). The optimum concentration of oxygen was 0.01 kPa (oxygen concentration varied from 0 to 0.1 kPa, see Figure S1 in Supporting Information). Meanwhile, the oxygen concentration almost remained unchanged during reaction below 250°C. With further increasing the temperature, the consumed oxygen (ca. 10%) could react with the surface carbon species and form carbonates or CO_2.

On the basis of the variation of the production of ethylene and formaldehyde, together with previous studies,[10,11] we hypothesize that ethylene is probably produced through the coupling of formaldehyde. The TPD-HCHO spectra from the oxygen precovered α-Mn_2O_3 nanocrystals (Figure 4a) in the temperature range of 25–400°C showed a broad desorption peak of ethylene centered at 175°C; a CO_2 desorption peak appeared around 338°C. In addition, almost no formaldehyde or other species was detected in the effluents, indicating that the adsorbed formaldehyde was completely reacted. For comparison, this experiment was conducted on

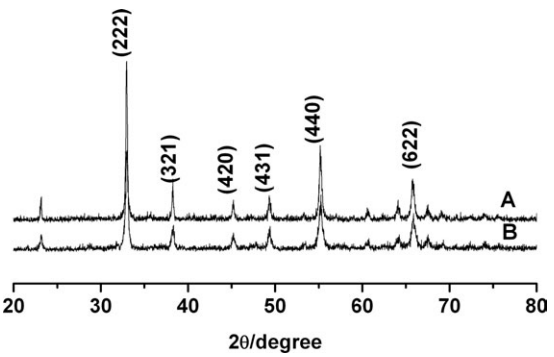

Figure 2. XRD patterns for the bulk α-Mn_2O_3 (A) and nanocrystal α-Mn_2O_3 (B).

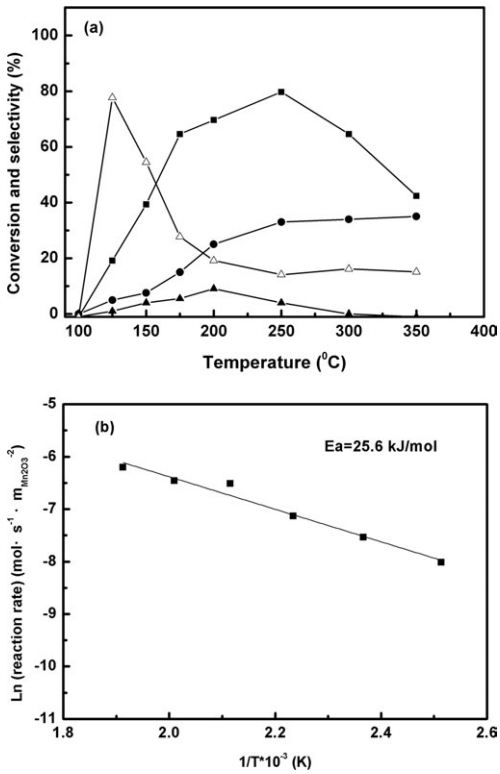

Figure 3. (a) Temperature-dependent MTO reaction on the α-Mn_2O_3 nanocrystal catalyst.

(●) Conversion of methanol, (■) selectivity to ethylene, (▲) selectivity to formaldehyde, and (△) selectivity to CO_2. Reaction conditions: 10.0 kPa CH_3OH, 2.6 kPa H_2O, 0.01 kPa O_2, and remaining He, with space velocity of 60,000 h^{-1} under atmospheric pressure. (b) Arrhenius plot of ethylene production by CH_3OH in a temperature range of 125–250°C with the initial rates (5 min), GHSV: 60,000 h^{-1}, the catalyst was diluted with α-Al_2O_3 by a ratio range of 1–5.

the same catalyst without preadsorbing oxygen. Similar to the spectrum shown in Figure 4a, an ethylene peak was observed at 175°C (Figure 4b); however, the amount of desorption was only about 10% compared with that shown in Figure 4a. Other peaks were observed including broad CO_2 and HCHO peaks centered at 275 and 170°C. Those spectra indicate the formation of ethylene through formaldehyde coupling, which is obviously favored by the preadsorbed oxygen. More interestingly, under the same conditions no ethylene could be detected (Figure 4c) over the bulk α-Mn_2O_3.

Ethylene production was further investigated in feedstock of formaldehyde over the oxygen-preoccupied α-Mn_2O_3 nanocrystal catalyst. Ethylene was confirmed to be the primary product in a typical experiment conducted at 150°C (Figure 5a). Noting that by mass spectroscopy (MS) signal at $m/e = 32$, a trace amount of oxygen probably from desorption was also measured. Formaldehyde conversion at 25 s (Figure 5b) was as high as about 45%, corresponding to an ethylene yield of 15%, but it declined with the time. Moreover, the selectivity of ethylene was about 66% initially and remained about 56% after 350 s. Complete deactivation occurred only after 400 s. The initial selectivity is close to the theoretically maximum value of about 66% according to Eq. 5. Consecutive experiments proved that the deactivated catalyst could be fully recovered through a simple regeneration process by removing the carbonyl residuals from the surface and readsorbing oxygen (Figure 5c). More interestingly, it was found that almost no CO_2 was detected during reaction, possibly owing to the formation of surface carbonates by adsorbing CO_2. Moreover, in the temperature range of 30–150°C, the initial reaction rate increased with the temperature; however, as depicted in Figure 5d, the rate decreased steadily with continuously increasing the temperature to 170°C. The Arrhenius plot (Figure 5d) yields an apparent activation energy (E_a) of 5.7 kJ mol^{-1}, suggesting that the energy barrier for this reaction is extremely low. Ethylene production was also qualitatively confirmed with an online rapid-response micro-gas chromatography instead of MS; similarly, ethylene was the only product detected at 150°C.

To gain deep insight into the deactivation mechanism, TPSR experiment was then performed on a spent catalyst resulting from the experiment in Figure 5a. A CO_2 peak

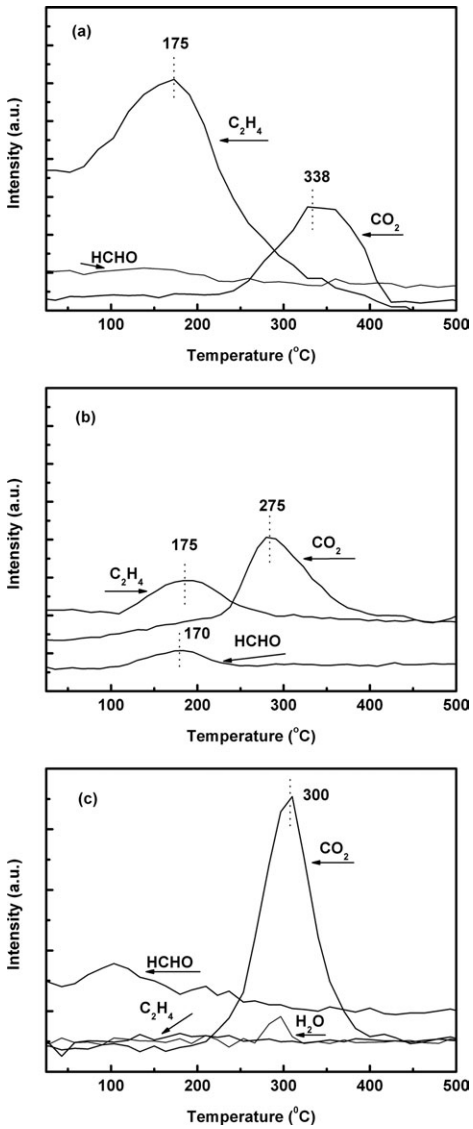

Figure 4. HCHO-TPD spectra obtained from oxygen-precovered α-Mn_2O_3 nanocrystal catalyst (a), α-Mn_2O_3 nanocrystals catalyst without preadsorbing oxygen (b), and oxygen-precovered bulk α-Mn_2O_3 (c).

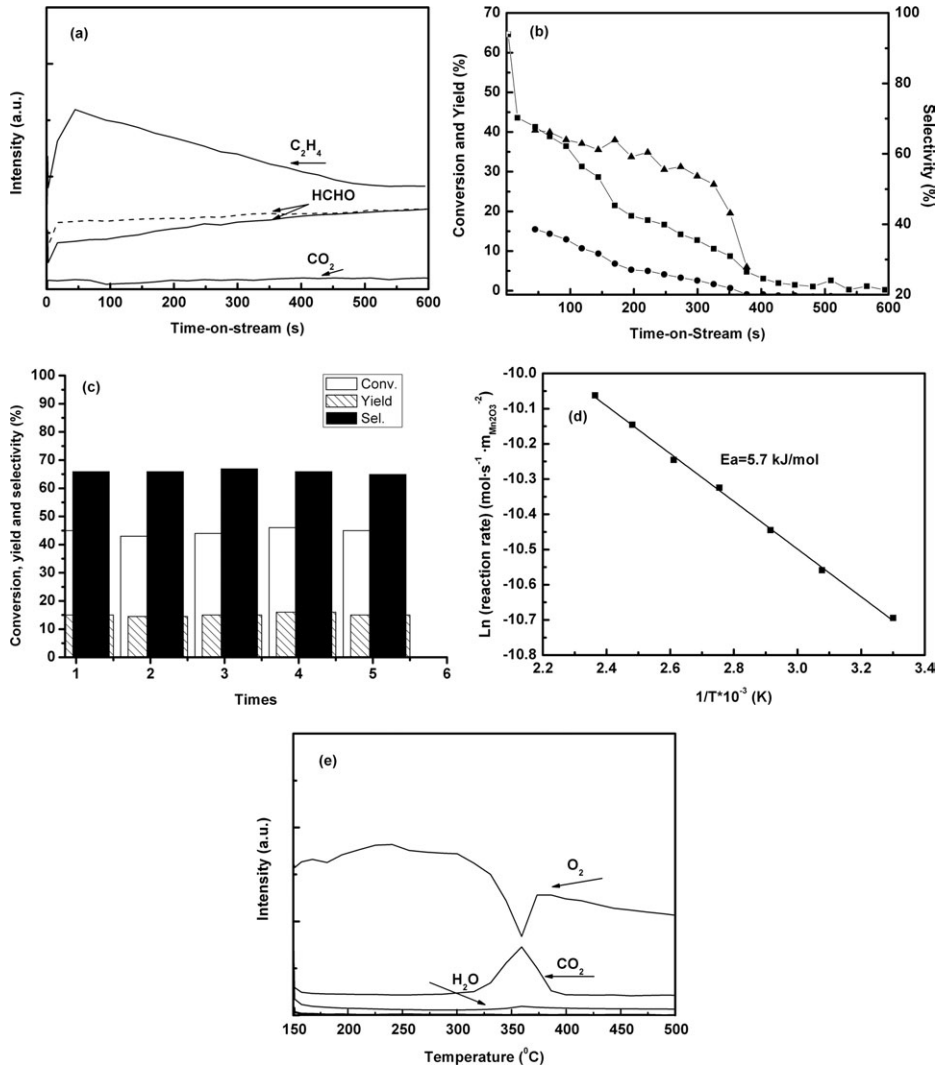

Figure 5. (a) Formaldehyde coupling on the α-Mn_2O_3 nanocrystal catalyst at 150°C in the presence of HCHO (0.14 kPa HCHO, 2.6 kPa H_2O, and remaining He), GHSV: 60,000 h^{-1}.

Solid line: time-dependent signals recorded in the reaction; dash line: time-dependent HCHO signal for reference, obtaining from a catalyst-free system. (b) Time-dependent conversion of HCHO (■), yield of ethylene (●), selectivity to ethylene (▲). Data were derived from the experiment in (a). (c) Ethylene production by formaldehyde coupling on the regenerated oxygen-precovered α-Mn_2O_3 nanocrystal catalyst, which, the catalyst was regenerated after 10-min reaction, following the procedure of preparing oxygen-precovered surface [in a O_2(5%)–He flow of 50 ml min^{-1} at 500°C for 1 h then cooling down to 150°C for reaction] under the same reaction conditions as (a); the data were taken at 25 s. (d) Arrhenius plot of ethylene production by HCHO coupling in a temperature range of 30–150°C, the initial rates (25 s) were calculated based on the conversion of HCHO (0.14 kPa HCHO, 2.6 kPa H_2O, and remaining He), GHSV: 60,000 h^{-1}. (e) TPSR spectra for the spent catalyst from experimental (a), O_2 (5.0 kPa O_2 and remaining He) flow rate of 50 ml min^{-1}, ramping rate of 20°C min^{-1}.

appeared at about 360°C in the O_2 flow (5.0 kPa O_2 in He; Figure 5e), indicating the combustion of the surface species such as carbon. The formation of unburn species during reaction may prevent the active sites from adsorbing formaldehyde molecules or coupling surface species. Another reason responsible for the deactivation is due to the loss of the weakly adsorbed oxygen (WAO), especially at elevated temperatures. The relevant issue will be discussed later. For comparison, the TPSR experiments were also carried out in a mixture of formaldehyde and oxygen on the oxygen-precovered α-Mn_2O_3 nanocrystals. However, only CO_2 was detected due to the complete oxidation of formaldehyde starting at 350°C (Figure 6).

To further elucidate the surface species configuration and the possible pathways for the surface reactions, we examined the vibrations of formaldehyde on the oxygen-precovered α-Mn_2O_3 nanocrystal surface through *in situ* DRIFTS (Figure 7). The bands at 3000, 2937, 2895 ($\nu_{(as)CH_2}$), 2855, 2837, and 2779 ($\nu_{(s)CH_2}$) cm^{-1} observed at room-temperature can be assigned to the different C—H stretching vibrations.[18–22] Meanwhile, several weak bands at 1587 (δ_{CH_2}), 1374, 1359 (ω_{CH_2} or ν_{CO}), 1138, 1110, and 1053 (γ_{CH_2} or ν_{CO}), and 1034 (O_2^-) cm^{-1} were also observed (Figure 7b). The intensities for those bands dropped drastically at above 150°C because of the coupling and desorption of surface species. On the other hand, formaldehyde molecules are assumed to be dissociated immediately after adsorption, because the bands in the region of 1725–1745 cm^{-1}, which is usually assigned to the C=O bond in free or weakly adsorbed formaldehyde molecules,[20] were not detectable. Nevertheless, the

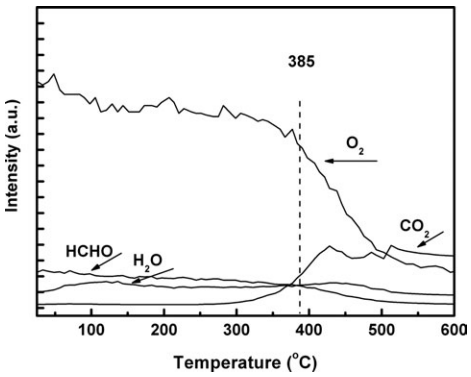

Figure 6. TPSR spectra obtained from the oxygen-precovered α-Mn_2O_3 nanocrystal catalyst.

Reaction conditions: a stream of 0.14 kPa HCHO, 5.0 kPa O_2, 2.6 kPa H_2O, and remaining He, a total flow rate of 50 ml min^{-1}, catalyst amount of 50 mg, and ramping rate of 20°C min^{-1}.

assignments here are open to discuss as the vibration spectra for the adsorption and transformation of formaldehyde on manganese oxides have not been available yet.

It is generally accepted that there are two reactions occurring for the adsorbed formaldehyde molecules on the surfaces of metal oxides: oxidation [producing surface formate ($HCOO_{(a)}$)] and cannizaro-type disproportionation [producing surface formate ($HCOO_{(a)}$) and methoxide ($CH_3O_{(a)}$)]. The DRIFT spectra demonstrated the existence of abundant $CH_{2(ad)}$-containing species derived from the adsorption of formaldehyde, which are responsible for the formation of ethylene through coupling. We propose the reaction may proceed through a four-member ring intermediate by bonding two double bonds with adjacent Mn atoms on the catalyst surface, as rationalized by Eq. 5. On the other hand, dioxymethylene ($H_2COO_{(a)}$) produced by nucleophlilic attack of surface oxygen atoms at carbonyl carbon[18–20] may lead to the formation of formic acid or carbonates. The band at 1034 (O_2^-) cm^{-1} (Figure 7b) hints that the oxygen atom in formaldehyde molecule may also transfer into oxygen anions bonding to Mn during the coupling reaction. Those oxygenates may further convert into carbonate or oxygen molecule through a redox process.

$$3HCHO \rightarrow C_2H_4 + CO_2 + H_2O \quad \Delta G^{\circ}_{f\,298\,K} = -246.6 \ \text{(kJ mol}^{-1}\text{)} \tag{5}$$

The surface oxygen has proved to enhance the formaldehyde coupling reaction significantly. As mentioned above, the oxygen-precovered α-Mn_2O_3 nanocrystals are particularly active and selective for formaldehyde coupling to produce ethylene at/below 150°C. The catalyst deactivated drastically above 175°C is owing to the loss of the preadsorbed oxygen species as the catalyst surface was covered with carbon deposits, which blocked the adsorption of oxygen. Another reason could be that the loss of WAO may result from the thermal desorption. We have shown recently that the WAO on manganese oxides[21,22] such as α-Mn_2O_3 crystals could be active species in catalytic reactions such as CO oxidation under mild conditions, even though the elemental steps about this reaction are still not clear. On the other hand, the α-Mn_2O_3 nanocrystals displayed higher capacity to oxygen adsorption than the bulk as evidenced by the O_2-TPD spectra. As shown

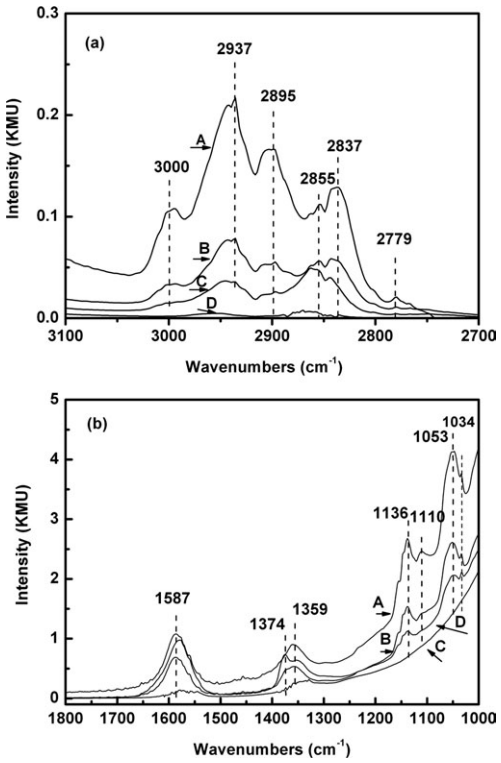

Figure 7. *In situ* DRIFT spectra measured at various temperatures for the adsorption of HCHO on the oxygen-precovered α-Mn_2O_3 nanocrystal catalyst.

(a) The region of 3100–2700 cm^{-1} and (b) the region of 1800–1000 cm^{-1}. (A) 30°C, (B) 50°C, (C) 150°C, (D) α-Mn_2O_3 nanocrystal in a HCHO-free system at 30°C.

in Figure 8, three peaks at 135, 200, and 300°C were identified for the α-Mn_2O_3 nanocrystals (curve B). The first two peaks may be resulted from the WAO and the third one from the lattice oxygen. It is noteworthy that the temperature for completely desorbing WAO (at 200°C) is almost close to that for deactivation. In contrast, only one desorption peak at 450°C, possibly from the lattice oxygen, was observed for the bulk (curve A), the peak area was about 5% of the one for the α-Mn_2O_3 nanocrystals. Low capability for adsorbing oxygen is

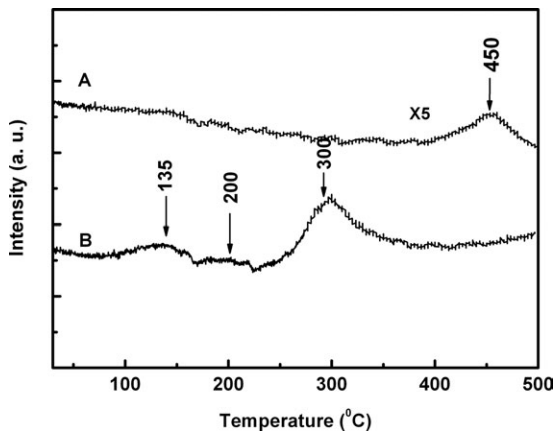

Figure 8. O_2-TPD spectra for the oxygen-precovered (A) bulk α-Mn_2O_3 and (B) α-Mn_2O_3 nanocrystal with a N_2 flow rate of 50 ml min^{-1}, ramping rate of 20°C min^{-1}.

perhaps the main reason for the poor activity measured for the bulk. Most likely, the surface structure of the catalyst, for example, the Mn—Mn bond distance, can be finely tuned by the WAO and, thus, reconstructed surface favors —CH_2 coupling. Interestingly, the adsorbed oxygen on pure metal surfaces has proved to lead to the polymerization of formaldehyde,[23–25] but it has never been reported on metal oxide surfaces.

We also need to mention that in the presence of gas-phase oxygen, the reaction route may be altered as there was no ethylene or other carbon species but CO_2 detected above 350°C (Figure 6). It is likely that the surface is saturated with adsorbed oxygen and/or carbonyl species that may suppress the adsorption of formaldehyde molecules or prevent the surface species from coupling. Moreover, the extra absorbed oxygen species may cause the complete oxidation of ethylene.

It should be pointed out that ethylene produced through formaldehyde coupling on the α-Mn_2O_3 nanocrystal catalyst is reported for the first time, even though the adsorption/reaction of formaldehyde have been studied on various polycrystalline and single crystal oxides surfaces.[18,20] Several reactions have been identified by the HCHO-TPD spectra. Among them, a trace amount of ethylene, acetylene, and formic acid was detected in effluents using TiO_2 powder[12] and $UO_2(111)$.[13]

Water in this system comes from the reaction and feedstock by bubbling may affect also the adsorption/desorption of reactants during reaction. The exact role of water in this reaction system is still elusive. We believe the weak bonding for water on metal oxide surfaces would remarkably change the reaction mechanism. More experiments with this respect are underway.

Our experimental results strongly suggest that the α-Mn_2O_3 nanocrystals can be a potential catalyst for the MTO reaction. It shows higher selectivity toward ethylene. The reaction follows a possible reaction route of methanol → formaldehyde → ethylene. However, the maximum selectivity of 80% toward ethylene in MTO is higher than 66% calculated for formaldehyde coupling, it manifests that more than one pathway should be responsible for MTO in this system. Nevertheless, this study has provided evidences not only for the design of new MTO catalysts but also for the theoretic study of this reaction system on metal oxide catalysts.

Conclusions

We have shown that ethylene production through the MTO reaction could be achieved on an α-Mn_2O_3 nanocrystal catalyst, while formaldehyde coupling was one of the intermediate reactions. The conversion reached to 35% at 250°C with the maximum selectivity of 80% toward ethylene in MTO, while formaldehyde conversion of 45% and selectivity of 66% toward ethylene were measured at 150°C through formaldehyde coupling. The present results suggest that metal oxide catalysts can be potential alternatives for the MTO reaction.

Acknowledgments

The authors are grateful to the support from the Chinese Education Ministry 111 project (B08021), the National Science Foundation (21006068, 21176071, 21106041), the Program for New Century Excellent Talents in University (NCET-10-0611), and the Program of Introducing Talents of Discipline to Universities (B06006), Shanghai PuJiang Talent Program (2010/10PJ1402500, 2011/11PJ1402400), Program of Science and Technology Commission of Shanghai Municipality (11JC1402700), Innovation Program of Shanghai Municipal Education Commission (11ZZ52, 11ZZ051), Shanghai Natural Science Foundation (11ZR1408400), Shanghai Key Laboratory of Molecular Catalysts and Innovative Materials (Fudan University) (2010MCIMKF01), Creative Team Development Project of Ministry of Education (IRT0721) and Fundamental Research Funds for the Central Universities.

Notation

ΔG°_{f298K} = free energy, kJ mol^{-1}
S_{BET} = surface area, m^2 g^{-1}
d_p = mean particle size, nm
D = crystal size, nm
$r_{CH_3OH/HCHO}$ = reaction rate based on CH_3OH/HCHO conversion, mol s^{-1} · $m_{Mn_2O_3}^{-2}$
$m_{Mn_2O_3}$ = mass of α-Mn_2O_3 in the reactor bed
V_{gas} = total molar flow rate, ml min^{-1}
$X_{CH_3OH/HCHO}$ = conversion of CH_3OH/HCHO based on ethylene formation, %
$c_{CH_3OH/HCHO}$ = concentration of CH_3OH/HCHO in gas mixture, %

Greek letters

$\nu_{(as)CH_2}$, $\nu_{(s)CH_2}$,δ_{CH_2}, ω_{CH_2},ν_{CO}, and γ_{CH_2} = different vibrational mode of surface species

Abbreviations

DRIFTS = diffuse reflectance infrared Fourier transform spectroscopy
GC–MS = gas chromatography–mass spectroscopy
MTO = methanol-to-olefin
POM = partial oxidation of methane
SEM = scanning electronic microscopy
TPD = temperature-programmed desorption
TPSR = temperature-programmed surface reaction
WAO = weakly adsorbed oxygen
XRD = X-ray diffraction
H-ZSM-5 = hydrogen-zeolite socony mobile-5
QMS = gas chromatograph-quadrupole mass spectrometer
PID = proportion integration differentiation
HPLC = high performance liquid chromatograph
TPO = temperature-programmed oxidation
SAPO = silicoaluminophosphate

Literature Cited

1. Van Santen RA, van Leeuwen PWNM, Moulijn JA, Averill BA. *Catalysis: An Integrated Approach*. Amsterdam: Elsevier, 1999.
2. Bodke AS, Olschki DA, Schmidt LD, Ranzi E. High selectivities to ethylene by partial oxidation of ethane. *Science*. 1999;285:712–715.
3. Pereira CJ. Method for converting methanol. *Science*. 1999;285:670–671.
4. Gayubo AG, Alonso A, Valle B, Aguayo AT, Bilbao J. Deactivation kinetics of a HZSM-5 zeolite catalyst treated with alkali for the transformation of bio-ethanol into hydrocarbons. *AIChE J*. 2012;58:526–537.
5. Gucbilmez Y, Dogu T, Balci S. Ethylene and acetaldehyde production by selective oxidation of ethanol using mesoporous V-MCM-41 catalysts. *Ind Eng Chem Res*. 2006;45:3496–3502.
6. van Dijk CP. Inventors. Process for recovering ethylene from an olefin stream produced by a methanol to olefin reaction. US patent 5,811,621, 1998.
7. Wu X, Abraha MG, Anthony RG, van Dijk CP. Inventors. WO patent 03/078359, 2003.
8. Cockman RW, Haining, GJ. Inventors. Process for the hydration of olefins. US patent 6,953,867, 2005.
9. Wang W, Jiang Y, Hunger M. Mechanism investigations of the methanol-to-olefine (MTO) process on acidic zeolite catalysts by in situ solid-state NMR spectroscopy. *Catal Today*. 2006;113:102–114.
10. Lesthaeghe D, van Speybroeck V, Marin GB, Waroquier M. The rise and fall of direct mechanism in methanol-to-olefin catalysis: an overview of theoretical contributions. *Ind Eng Chem Res*. 2007;46:8832–8838.
11. Tajima N, Tsuneda T, Toyama F, Hirao K. A new mechanism for the first carbon–carbon bond formation in the MTG process: a theoretical study. *J Am Chem Soc*. 1998;120:8222–8229.
12. Kecskés T, Raskó J, Kiss J. FTIR and mass spectrometric studies on the interaction of formaldehyde with TiO_2 supported Pt and Au catalysts. *Appl Catal A*. 2004;273:55–57.

13. Senanayake SD, Chong SV, Idriss H. The reactions of formaldehyde over the surfaces of uranium oxides: a comparative study between polycrystalline and single crystal materials. *Catal Today*. 2003;85: 311–320.
14. Han Y-F, Chen L, Ramesh K, Widjaja E, Chilukoti S, Surjami IK, Chen J. Kinetic and spectroscopic study of methane combustion over α-Mn_2O_3 nanocrystal catalysts. *J Catal*. 2008;253:261–268.
15. Han Y-F, Chen L, Ramesh K, Zhong Z, Chen F, Chin J, Mook H. Coral-like nanostructured α-Mn_2O_3 nanocrystals for catalytic combustion of methane. *Catal Today*. 2008;131:35–41.
16. Han Y-F, Ramesh K, Chen L, Widjaja E, Chilukoti S, Chen F. Observation of the reversible phase-tranformation of α-Mn_2O_3 nanocrystals during the catalytic combustion of methane by in situ raman spectroscopy. *J Phys Chem C*. 2007;111:2830–2833.
17. Ramesh K, Chen L, Chen F, Zhong Z, Chin J, Mook H, Han Y-F. Preparation and characterization of coral-like nanostructured α-Mn_2O_3 catalyst for catalytic combustion of methane. *Catal Commun*. 2007; 8:1421–1426.
18. Busca G, Lamotte J, Lavalley JC, Lorenzelli V. FT-IR study of the adsorption and transformation of formaldehyde on oxide surfaces. *J Am Chem Soc*. 1987;109:5197–5202.
19. Li C, Domen K, Maruya K-I, Onishi T. Spectroscopic identification of adsorbed species derived from adsorption and decomposition of formic acid, methanol, and formaldehyde on cerium oxide. *J Catal*. 1990;125:445–455.
20. Sheppard NT, Davydov A. *Molecular Spectroscopy of Oxide Catalyst Surface*. Chichester, UK: Wiley, 2003.
21. Han Y-F, Chen F, Zhong Z-Y, Ramesh K, Widjaja E, Chen L-W. Synthesis and characterization of Mn_3O_4 and Mn_2O_3 nanocrystals in the pores of ordered mesoporous silicas (SBA-15): novel combustion catalysts at low temperatures. *Catal Commun*. 2006;7:739–744.
22. Han Y-F, Chen F, Zhong Z-Y, Ramesh K, Chen L-W, Widjaja E. Controlled synthesis, characterization and catalytic properties of Mn_2O_3, Mn_3O_4 nanoparticles supported on mesoporous silica SBA-15. *J Phys Chem B*. 2006;110:24450–24456.
23. Zhou J, Mullins DR. Adsorption and reaction of formaldehyde on thin-film cerium oxide. *Surf Sci*. 2006;600:1540–1546.
24. Houtman C, Barteau MA. Reactions of formic acid and formaldehyde on Rh(111) and Rh(111)-(2x2)O surfaces. *Surf Sci*. 1991;248: 57–67.
25. Stuve EM, Madix RJ, Sexton BA. An EELS study of the oxidation of H_2CO on Ag(110). *Surf Sci*. 1982;119:279–290.

Manuscript received Sept. 26, 2011, and revision received Nov. 30, 2011.